Scientific Research Publishing

International Journal of Geosciences, 2024, 15, 1087-1112
https://www.scirp.org/journal/ijg
ISSN Online: 2156-8367
ISSN Print: 2156-8359

Using Gravity Data to Highlight Tectonic Faults with Filtering Techniques and Modelling at the Congo Craton-Pan-African Belt Contact, East Cameroon

Owono Amougou Olivier Ulrich Igor[1,2*], Ngoumou Paul Claude[3*], Mono Jean Aimé[4,5], Ngoa Embeng Steve[6], Bidichael Wahile[6], Gouet Daniel Hervé[7], Ndougsa Mbarga Theophile[6,8]

[1]Department of Environmental Engineering, National Advanced School of Public Works, Yaoundé, Cameroon
[2]Advanced School of Mines Processing and Energy Resources, University of Bertoua, Bertoua, Cameroon
[3]School of Geology and Mining Engineering, University of Ngaoundéré, Ngaoundéré, Cameroon
[4]Department of Basic Training, Higher Technical Teachers' Training College (ENSET), University of Douala, Douala, Cameroon
[5]Department of Textile and Clothing Industries, Higher Technical Teachers' Training College (ENSET), University of Douala, Douala, Cameroon
[6]Department of Physics, Faculty of Science, University of Yaoundé I, Yaoundé, Cameroon
[7]Department of Mine and Career, Faculty of Mine and Petroleum Industry, University of Maroua, Maroua, Cameroon
[8]Department of Physics, Advanced Teacher's Training College, University of Yaoundé I, Yaoundé, Cameroon
Email: *oaoulrich@gmail.com, *ngpclaude@yahoo.fr

How to cite this paper: Igor, O.A.O.U., Claude, N.P., Aimé, M.J., Steve, N.E., Wahile, B., Hervé, G.D. and Theophile, N.M. (2024) Using Gravity Data to Highlight Tectonic Faults with Filtering Techniques and Modelling at the Congo Craton-Pan-African Belt Contact, East Cameroon. *International Journal of Geosciences*, **15**, 1087-1112.
https://doi.org/10.4236/ijg.2024.1512057

Received: October 15, 2024
Accepted: December 24, 2024
Published: December 27, 2024

Abstract

The geological and tectonic impact of the collision between the Congo Craton and the Pan-African Ridge of Central Africa was considerable, with the formation of various tectonic faults, fractures, dykes and folds. The present gravity analysis is based on the analysis of EGM 2008 gravity data using different operators. Oasis Montaj software was used to process the data. The Bouguer anomaly map was used to identify the main local and regional anomalies. In addition, maps of the horizontal and vertical gradients of the Tilt angle analytical signal revealed several short-wavelength anomalies such as folds, dykes, fractures and faults. The map of superimposed maxima was used to create the structural map of the study area. For its part, the quantitative study provided an opportunity to assess the depths at which the anomalies originated. The deepest anomalies are more than 17 km deep and lie to the south of the study area. Examination of these various maps reveals that the various geological faults mentioned above generally follow ENE-WSW, ESE-WNW, NE-SW, NW-SE, E-W and even N-S directions. All of these directions appear to be closely linked to the geological history of the region. It is quite clear that the study area was the site of intense tectonic movements caused by the collision

between the Congo craton and the Pan-African chain of Central Africa.

Keywords

Faults, Lineaments, Contacts, Modelling

1. Introduction

The region that is the subject of this study is in the East of Cameroon. It covers an area of one square degree, and its geographical coordinates are 4˚N and 5˚N latitude North and 13˚E and 14˚E longitude East. Numerous geological and tectonic studies have revealed that Cameroon is characterised by two major litho-structural complexes, namely the Congo Craton in the south and the Central African Pan-African chain in the north. Folds, shears, fractures and faults are all present. Different structures of evolution and age are present, distributed from north to south between the Pan-African and Cratonic domains. Mapping the EGM 2008 gravity data is the objective of this study, which uses a multi-scale analysis.

In this study, therefore, a qualitative analysis will be carried out through the interpretation of the Bouguer anomaly map, the directional gradients, the analytical signal, the tilt angle and the multi-scale analysis on the one hand. On the other hand, a quantitative analysis through the determination of Euler solutions and $2^{3/4}$-D modelling.

2. Geological and Tectonic Context of the Study Area

There are several types of relief in the study area, including granitic relief, which presents domes in various forms, such as pitons, hills and rounded domes.

Figure 1 shows that the region is almost entirely covered by migmatites, granitic gneisses and granites, as well as micaschists and quartzites, according to the geological map by [1] and [2]. In agreement, the micaschists and quartzites are based on a gneissic and migmatitic substratum. The metamorphic assemblage is completely folded by synthesis, with dips ranging from subhorizontal to almost vertical. These rocks have all been exposed to Pan-African tectonics, with geochronological ages of 500 - 600 million years.

From a hydrogeological point of view, the ancient basement formations have a shallow hydrostatic level. Being mainly composed of granites and gneisses, these formations generally have classic arenas which do not pose any complex problems [2]. The more or less significant intercalations of quartzites in the schistose formations, as the weather, also create arenas. From a certain depth, granites, gneisses and migmatites are impermeable. There are, of course, no deep aquifers as in some sedimentary formations.

The geodynamic context of this zone is influenced by the collision between the Congo craton and the Pan-African chain. The Central Cameroon Shear (CCC) and the Sanaga fault cross the area [3]. The ductile to ductile-fragile shear (CCC)

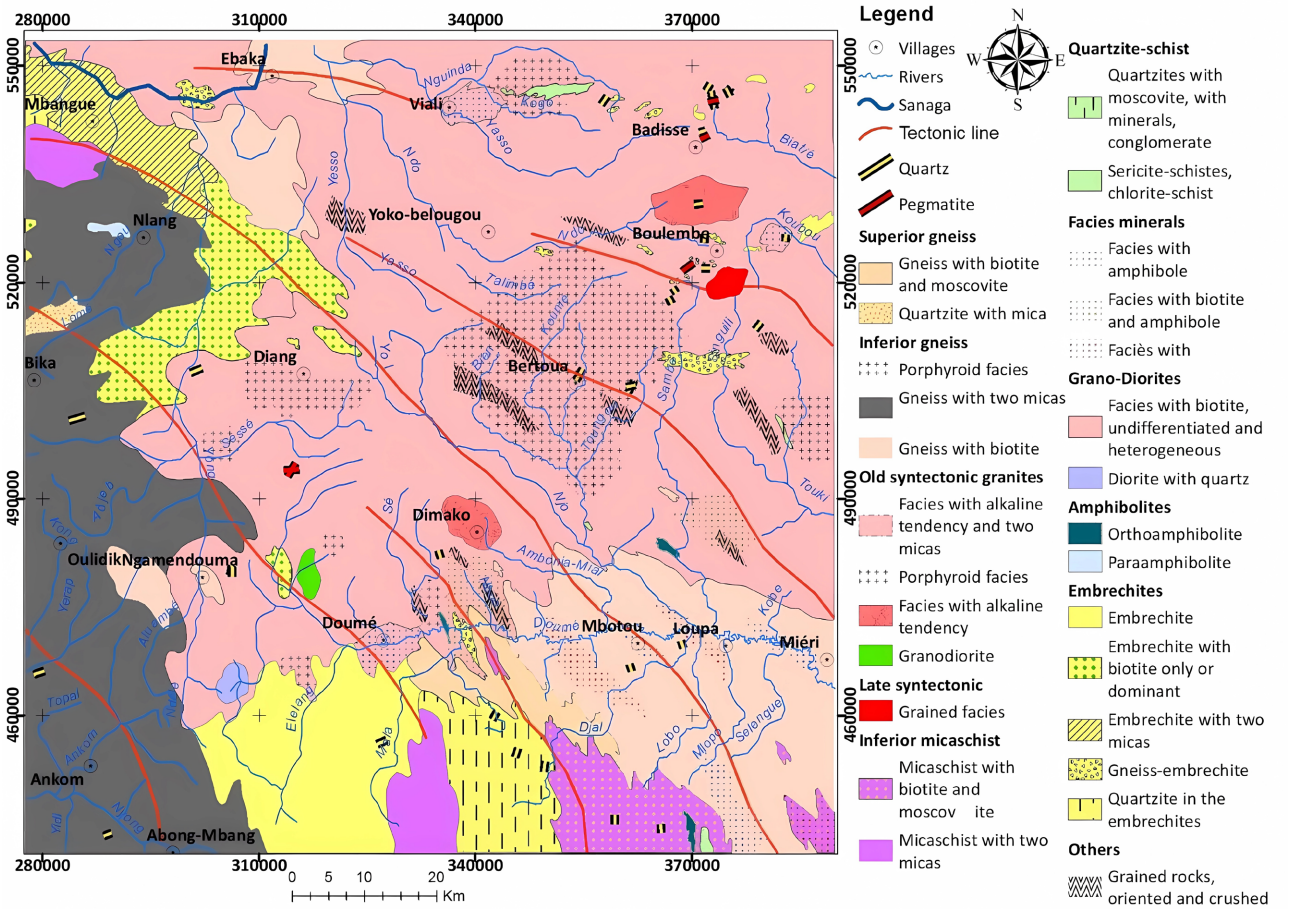

Figure 1. Geological map of the study area.

is one of the main elements of the Adamaoua tectonic fault, running ENE-WSW [4] [5]. The geological formations observed show multiple cycles. They were affected by three phases of Pan-African deformation, accompanied by metamorphic recrystallisation in amphibolite facies of high to low grade [6].

The subsoil here is fairly rigid. As a result, the tectonics are fragile, with an abundance of fissures. The old basement is bordered by fault fields or flexures [7]. Two types of accidents were caused by the intensity of the stresses: swellings caused by less intense tectonics and faults caused by more intense tectonic stresses [7].

Several studies show the presence in the central domain of high-grade gneisses of Palaeoproterozoic age (2100 Ma) intruded by syntectonic plutonites of Neoproterozoic age (550 ± 50 Ma) [8]-[12]. According to these authors, the area mentioned is ancient and continental, with a Palaeoproterozoic origin that is repeated in the Pan-African.

The geological reconnaissance work carried out by [13] highlighted several tectonic foliations and lines in Cameroon in general and at the regional scale of the study area. These foliations and tectonic lines are thought to be the result of the collision between the Congo Craton and the Pan-African Chain of Central Africa. This hypothesis was reinforced by the work of [14], who proposed a tectonometamorphic evolution that led to a collision model showing a boundary between these two units.

The geodynamic context of this zone is marked by the collision between the Congo Craton and the Pan-African chain. The Pan-African units were pushed onto the Craton as a result of this collision [15]-[17]. More than a hundred kilometres beneath the Yaoundé nappe, the Craton extends at depth [18]. Today, the boundary is an erosion boundary, and at the Pan-African level, the nappe largely covers the Craton to the south.

Located in the eastern part of Cameroon, the study area poses numerous geological problems due to the considerable gap between primary surface observations and a lack of sub-surface observations. Direct geological studies and geophysical surveys in the field are made difficult by the dense vegetation cover. However, potential field information is an essential source of information on subsoil geology and tectonic features.

3. Methodology

3.1. The Gravity Anomaly: Bouguer Anomaly

The Bouguer anomaly is the gravimetric response caused by heterogeneities in subsoil density [19]. In simple terms, it results from the difference between the gravity measurement that has undergone the Bouguer correction (Faye correction, plateau correction and relief correction) and the gravity value on the reference ellipsoid, at the vertical of the measurement station. Its expression is given by:

$$\Delta g_B = \left[g_{mes} + \Delta g_F - \Delta g_B + \Delta g_T \right] - g_{th}, \quad (1)$$

where: Δg_B is the Bouguer anomaly; g_{mes}, the value of g measured at station S on the topographic surface; Δg_F: the Faye correction; Δg_B: the simple plateau or Bouguer correction; Δg_T: the topographic correction; and g_{th}: the value of g calculated on the ellipsoid (E) plumb with S.

3.2. Derivatives

Derivation filters amplify the effect of shallow sources by attenuating the effect of deep ones, focusing on anomalies and making it possible to better define the geometric limits of bodies.

3.2.1. The Horizontal Gradient

The horizontal gradient is used to identify contacts that may be faults, fractures, or lithological boundaries in magnetic or gravity data. These contacts are very intense [20] [21]. This method has the advantage of not being affected by noise emitted by the data during the aeromagnetic or gravity survey, as it only takes into account the first derivatives of the magnetic field in the horizontal plane [22]. The horizontal gradient of a magnetic or gravimetric field M, also known as the HGM, is calculated by studying the horizontal derivatives in the x and y directions. We therefore have:

$$HGM(x,y) = \sqrt{\left(\frac{\partial M}{\partial x}\right)^2 + \left(\frac{\partial M}{\partial y}\right)^2} \quad [22] \quad (2)$$

If the following assertions are met, this function provides maxima over

geological contacts. The regional magnetic field must be vertical or horizontal depending on the position on the earth's surface.

- The magnetisation must follow the same direction as the regional field.
- Geological contacts must be vertical and well insulated.
- Magnetic sources must be thick.

When the first four assertions are violated, the local maxima are displayed on the map above the contacts, while violation of the fifth creates a second maximum parallel to the contact. In order to resolve these difficulties, it is necessary to convert the data using the pole reduction operator. The analytical signal, which does not depend on the directions of the magnetisation and the magnetic field, will make it possible to determine the definitive geological contacts.

3.2.2. The Vertical Gradient

Short-wavelength anomalies are amplified by the vertical derivative, making it possible to locate the impact of surface structures in the subsurface by attenuating the impact of long-wavelength anomalies. Mapping the vertical gradient is essential for structural analysis of the study [23] [24] provided the algorithm to determine this gradient for a magnetic field *M*.

$$M(u,v) = M(u,v)\left(\left(u^2+v^2\right)^{\frac{1}{2}}/n\right)^n. \tag{3}$$

3.3. The Analytical Signal

According to [25]-[27], the analytical signal method is used to determine the depths and coordinates of magnetic sources. The special feature of the analytical signal is its ability to be independent of the direction of magnetisation of the source, given that the magnetic field is a vector whose direction and intensity vary according to the time and place of observation. According to [28], the amplitude of the analytical signal is directly linked to the value of the magnetisation. According to the research carried out by [29], the amplitude of the analytical signal is calculated by studying the squares of the derivatives of the total magnetic field as a function of the x, y and z directions. Its definition is given by:

$$|A(x,y)| = \sqrt{\left(\frac{\partial M}{\partial x}\right)^2 + \left(\frac{\partial M}{\partial y}\right)^2 + \left(\frac{\partial M}{\partial z}\right)^2}, \tag{4}$$

where M is the total magnetic field.

3.4. The Tilt-Angle Derivative

The Tilt-angle transformation calculates the inverse of the tangent of the ratio of the modulus of the horizontal gradient with the vertical gradient of the gravity field [30] [31] [32]. The equation for this transformation is written:

$$\theta = tan^{-1}\frac{\dfrac{\partial M}{\partial z}}{\sqrt{\left(\dfrac{\partial M}{\partial x}\right)^2 + \left(\dfrac{\partial M}{\partial y}\right)^2}}, \tag{4}$$

where M represents the gravity field. The values of the tilt angle are between $\frac{-\pi}{2}$ and $\frac{\pi}{2}$, this method delimits the variations in the amplitude of the angle within a certain range. The advantage of the transformation is that by calculating an angle, all the shapes will be represented in a similar way, whether the anomalies are small or large in amplitude [33]. The magnitude of the tilt angle is positive for gravity sources, almost zero at the edges of these sources, and negative outside of these magnetic sources [34]. This operator is applied to the Bouguer map.

3.5. Multi-Scale Analysis of Horizontal Gradient Maxima

Upward extension and horizontal gradient are two methods used in multi-scale analysis. The use of a multi-scale analysis is an effective means of locating in the subsurface the linear contacts corresponding to faults and the circular contacts representing the limits of intrusive bodies [35], on the one hand, and evaluating their trajectory, inclination and even their importance [36] [37], on the other. Indeed, the line indicating the local maxima of the values of this gradient highlights the boundary between two blocks with different densities or susceptibilities.

A curve representing the magnetic or gravimetric anomaly above a vertical contact shows a minimum on the side of rocks with low densities or susceptibilities and a maximum on the side of rocks with high susceptibilities. The point of inflection of the curve is at the vertical contact, which represents the maximum of the horizontal gradient [20] [21].

3.6. Euler Deconvolution

This is a filtering technique which allows the origins of anomalies to be identified. [38] [39] represents the total magnetic field intensity at the observation point P: $f\left[\left(x-x_0\right),\left(y-y_0\right),\left(z-z_0\right)\right]$ [20] [40] developed the homogeneity equation, which takes the following form:

$$\frac{\left(x-x_0\right)\partial M}{\partial x}+\frac{\left(y-y_0\right)\partial M}{\partial y}+\frac{\left(z-z_0\right)\partial M}{\partial z}=N\left(B-M\right), \tag{5}$$

where (x, y, z) are the coordinates of the observation point, $\left(x_0,y_0,z_0\right)$ are the coordinates of the magnetic source. The total magnetic field at the observation point is M, the regional value of the total magnetic field is B and the structural index N is used to define the type of source and the rate of change of the field as a function of distance. Euler deconvolution is based on solving the previous equation, which has four unknowns: x, y, z and B. Solving a system of equation with four unknowns requires four measurement points, and then the least squares method is used [23].

$N=-n$ is the structural index, where n represents the degree of homogeneity. It varies according to the shape of the source. Therefore, a homogeneous source with a structural index of $N=3$ is a linear source (such as a line of dipoles or poles, a homogeneous cylinder, a rod, etc.). In the case of $N=2$, the source is an

intrusive body such as a dyke, thin layer, etc. There is a contact when $N=1$, while a block is present at the top of a pyramid when $N=0$.

3.7. $2^{3/4}$-D Modelling

$2^{3/4}$-D modelling is based on three important parameters: the susceptibility or density contrast of the subsoil rocks, the depth of burial and the shape of the geological structures that are the source of the anomalies observed. The constraints on these parameters are derived from the geology of the study area and the analysis of magnetic or gravimetric data. The principle of this direct modelling method is to calculate the theoretical anomaly using a model of a simple structure such as a cylinder, sphere or prism, and compare it with the observed anomaly. The best model is the one that corresponds to the structure whose calculated anomaly is as close as possible by adjustment to the observed anomaly. However, the model selected should take geological clues into account as far as possible [41]-[43].

4. Results and Discussion

4.1. The Origin of the EGM-2008 Data

Researchers at the National Geospatial-Intelligence Agency (NGA) have developed the Earth gravity model known as EGM 2008 [44]. This model is a combination of terrestrial gravity data from Champ/Grace satellite data.

4.2. The Bouguer Anomaly Map

The various gravity anomalies identified are separated by zones of strong gradients, indicating the presence of density discontinuities that generally represent tectonic faults.

The map below (**Figure 2**) shows the Bouguer anomalies obtained with the EGM 2008 data. It shows several anomaly shapes. This map is characterised by a heavy anomaly (with a value greater than the average anomaly, *i.e.* −32 mGal) covering the south-western and central part (from Oulidik to Doumé) with a break-up to the north of Diang. This anomaly has an E-W to ESE-WNW direction in the West-Centre part and a N-S direction towards Diang. It has a long wavelength and appears to be bowl-shaped in the south-western part, while in the northern part, it has an ellipsoidal shape. This zone of heavy anomalies obviously indicates the presence of high-density materials such as granulites in the subsurface. This anomaly is thought to represent the gravity signature of a fault in the study area, which appears to be parallel to those observed on a regional scale and is thought to be the result of faults that acted as shear zones at the end of the Pan-African, and then during the Cretaceous.

- It is separated to the north-west (east of Mbangue) by a slight anomaly marked by very low values below −51 mGal. This anomaly appears to be elongated and trends N-S. The clear variation in gradients suggests a geological contact between several geological formations. This gravity anomaly appears to be linked

to the discontinuity highlighted in the work by [45] [46].

- The north-eastern part (the zone from Viali to Badissé) is also made up of light anomalies below −51 mGals; it is separated from the heavy anomaly mentioned above by intermediate anomalies. Its direction appears to be E-W. This anomaly corresponds to a local thickening of the structures created by depressions in the granitic basement.

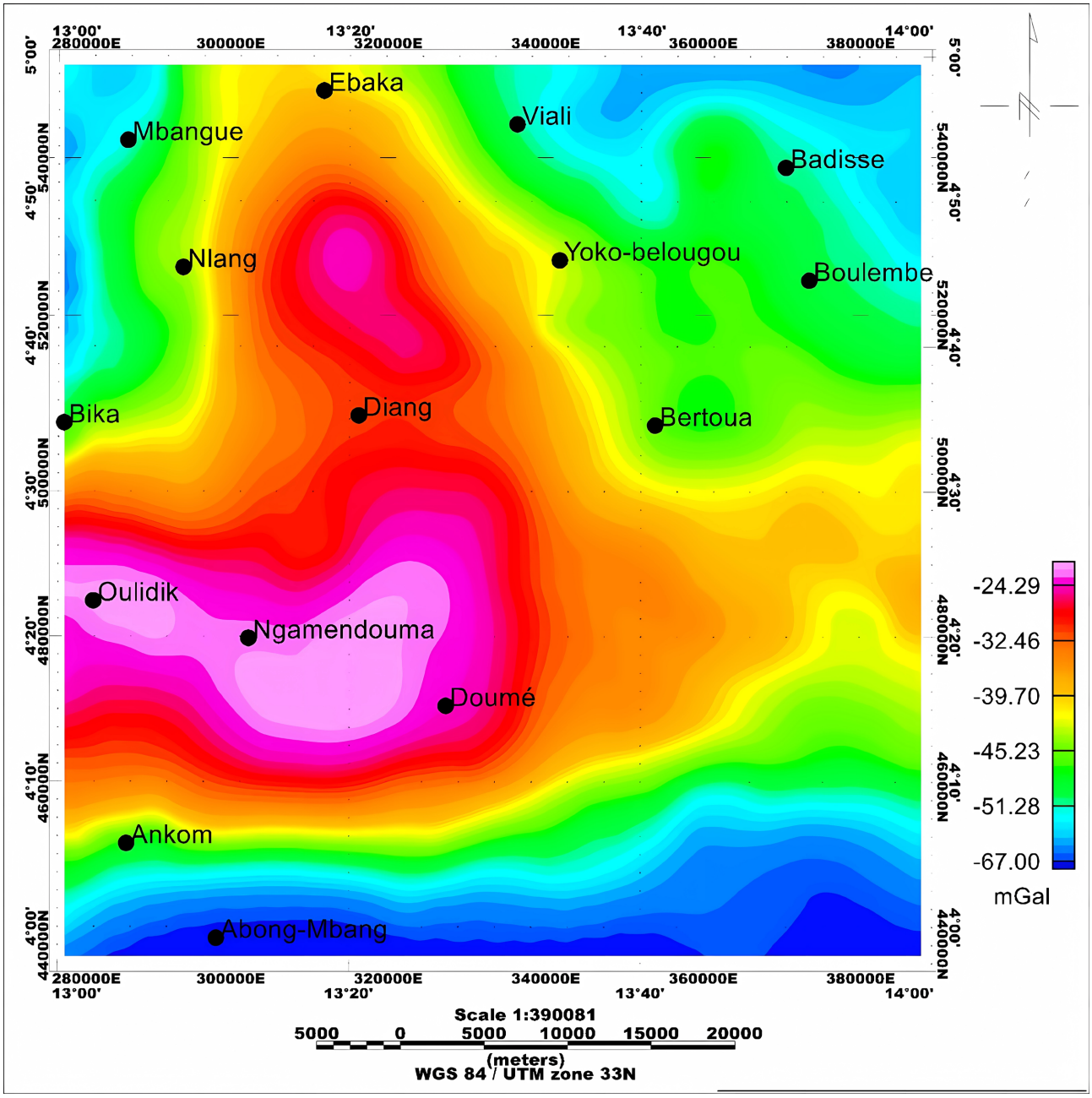

Figure 2. Map of Bouguer Anomalies.

- The central part of the map (south of Bertoua) is made up of medium anomalies with values between −32 mGals and −45 mGals. This anomaly is the continuation

of the previous heavy anomaly and is affected by the faults observed in the Pan African.

- The entire southern part is characterised by a light anomaly with values below −51 mGals. It appears to be sub-circular and oriented E-W. This anomaly is thought to reflect the effect of the formations bordering the Congo Craton.

The succession of positive anomalies and negative anomalies suggests that there have been accidents and/or clear contacts between lithological units that appear to be independent of one another.

4.3. The Vertical Gradient Map

The vertical derivative enhances the features of surface structures by amplifying short wavelength anomalies and attenuating the effect of long wavelength (low frequency) anomalies. This filter shows a lateral separation of anomalies and an amplification of the gravimetric effect of surface density contrasts to the detriment of depth contrasts.

The map below (**Figure 3**) shows anomalies along the Oulidik-Doumé axis that separate from east to centre and are characterised by a positive vertical gradient greater than 1.36 mGal/km. They trend ESE-WNW. In the same area, there is also a positive gradient anomaly that crosses the Ankom-Ngamendouma axis in an ENE-WSW direction. This anomalous zone is thought to be due to a dense mass upwelling that was observed on the Bouguer anomaly map. Similarly, to the north of Diang, there is an anomaly with a gradient greater than 1.36 mGal/km trending ESE-WNW, a direction recognised by the structures of the Adamaoua plateau and followed by the tectonic lines observed in the geological map of the study area. The area between Viali and Badissé to the north is also covered by a similar anomaly.

The southern part consists of an anomaly with a very low gradient (less than −1.63 mGal/km) in an E-W direction, characterising the presence of weakly dense structures, which are in agreement with the results obtained in the Bouguer anomaly map. The Mbangue zone also has an anomaly with a very weak gradient (less than −1.63 mGal/km) in a NE-SW direction. This could be linked to the passage of the Sanaga River through the area. The depression observed in the Viali area in the Bouguer anomaly map is well individualised in the present map. It follows the ENE-WSW direction.

This map also highlights two major corridors of sub-vertical and sub-horizontal positive gradient anomalies that pass almost through the centre of the study area. These anomalies could represent the transition between the two main units, the Congo Craton and the Pan-African Central African Chain.

4.4. The Analytical Signal Map

The analytical signal is a transformation that highlights shallow anomalies. It highlights the major tectonic directions and makes it possible to limit contacts

between geological formations by their density contrast and to expose intrusive bodies [38].

The map of the analytical signal above (Figure 4) highlights three major sectors with strong gradients, notably the South-West sector (Oulidick, Ankom, Abong-Mbang, Doumé), and the Nlang and Viali sectors.

The South-West sector has an E-W to ENE-WSW direction, characteristic of regional anomalies. The Vilali-Nlang magnetic zones are separated by anomalies with intermediate gradients, and trend ENE-WSW. This gives the impression that they formed a single block that was separated by a tectonic event of Pan-African age.

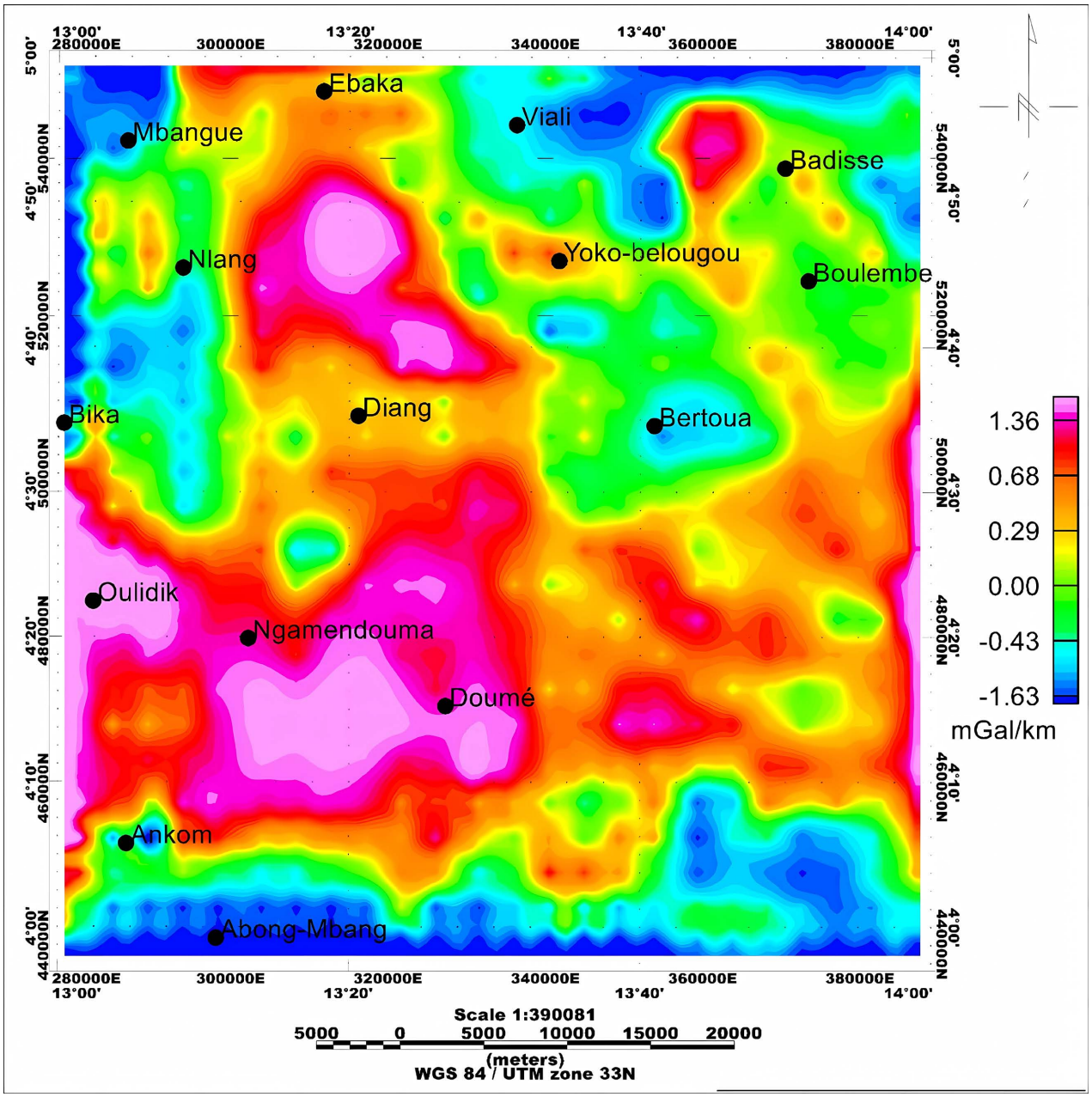

Figure 3. Vertical gradient map.

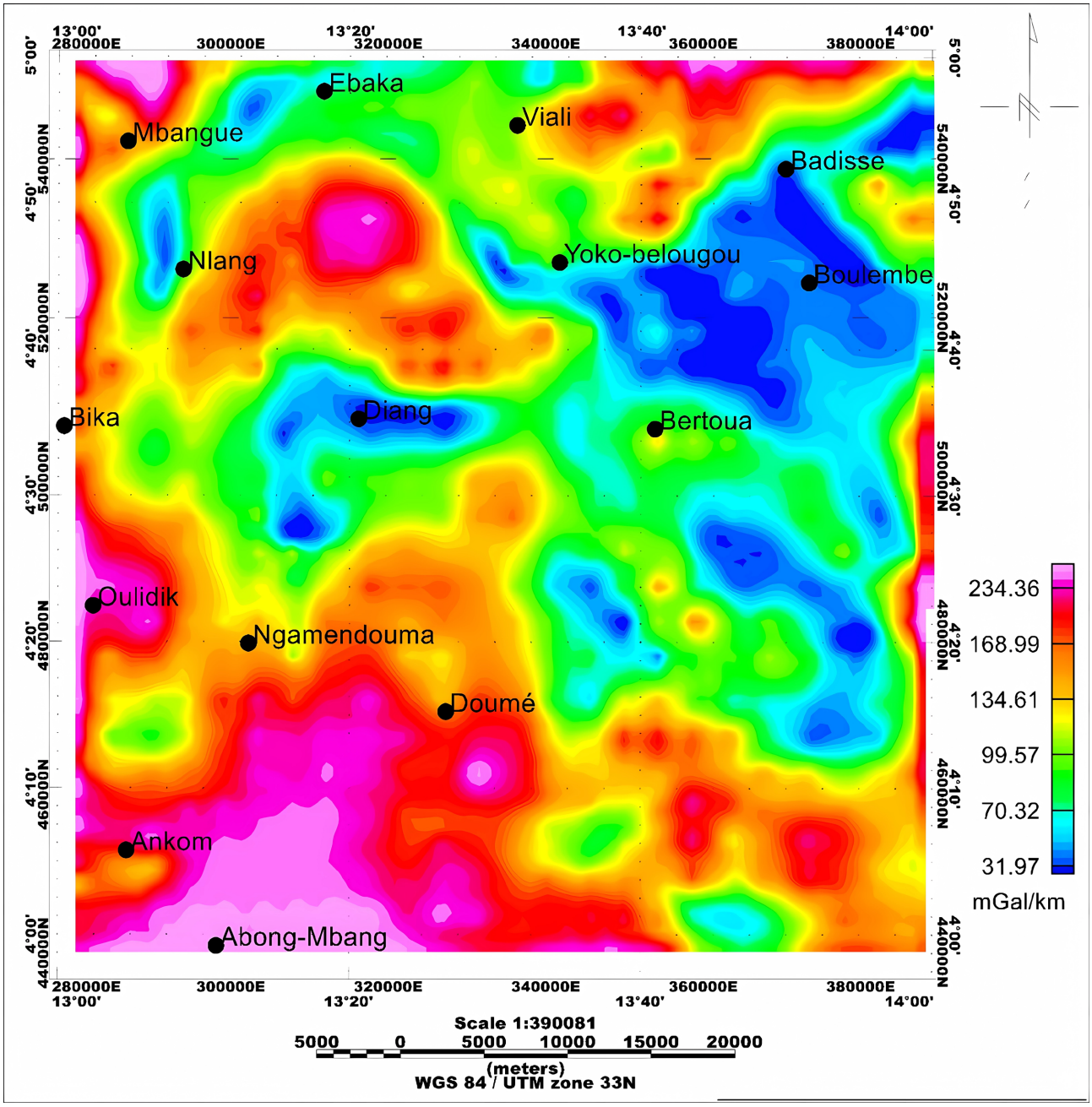

Figure 4. Analytical signal map.

4.5. The Tilt Angle Map

The map in **Figure 5** shows the dip angle anomaly, which highlights the intersecting lineaments and dykes. The orientations of the structures mentioned in the previous maps are clearly visible, which only confirms the results given above.

The Oulidik-Doumé fault still stands out, as do the regional E-W and N-S trending anomalies identified on the vertical gradient map, proving that these anomalies represent regional geological faults probably associated with subduction of the Pan-African in the Congolese Craton.

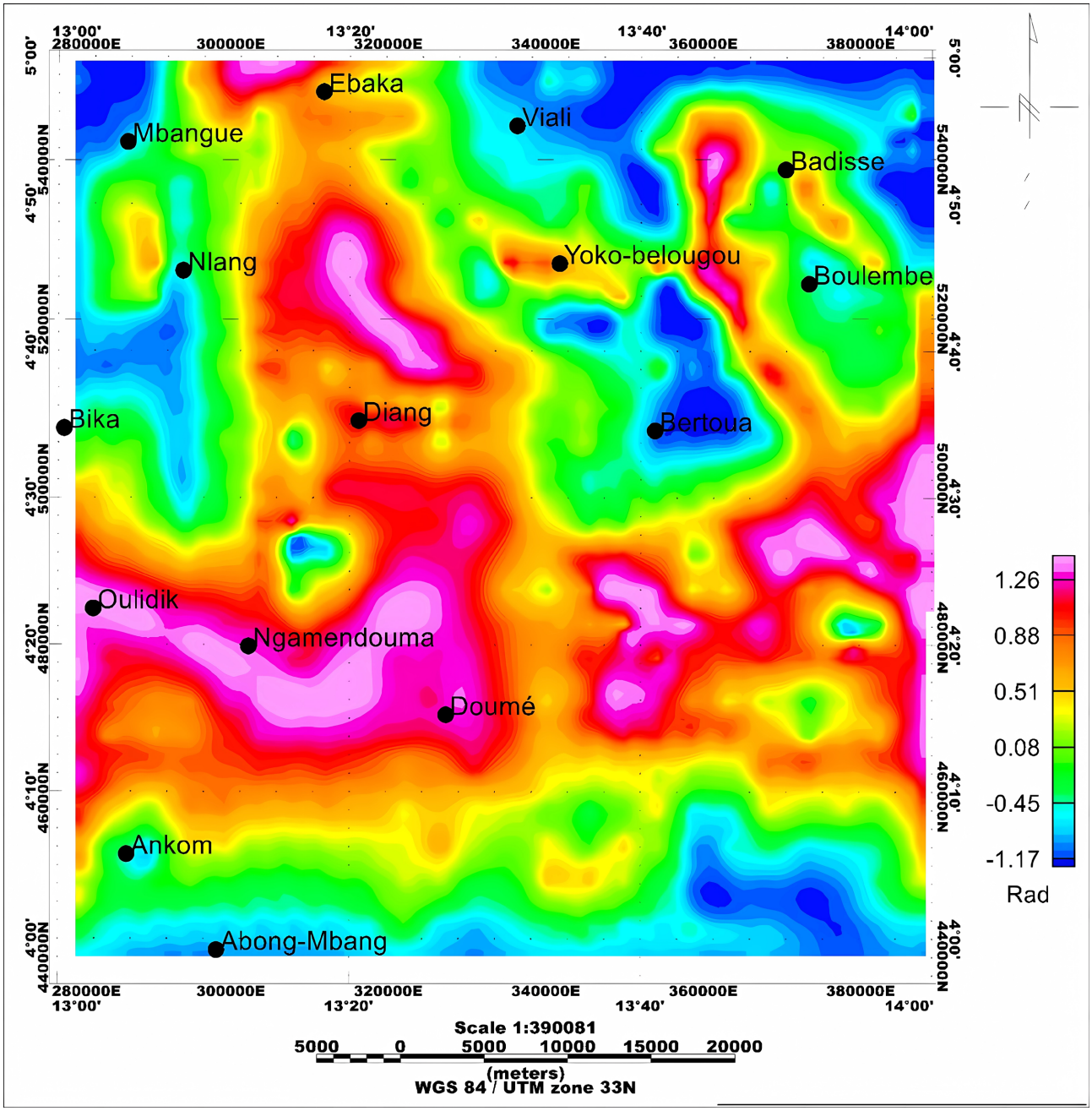

Figure 5. Tilt angle anomaly map.

4.6. Superimposed Maxima of the Horizontal Gradient

The map below (**Figure 6**) shows local maxima of the horizontal gradient extended upwards at several altitudes, in particular 10 km, 20 km and 30 km. According to Blakely & Simpson (1986), this superposition of maxima highlights the geological contacts associated with the faults or fractures suspected in the previous maps. This method also highlights the direction of dips. Vertical dips will show a superimposition of maxima, while oblique dips will show a shift of maxima in the direction of dip. This reveals a structural complexity marked by the alignment of

maxima, indicating the existence of several linear structures that have affected the basement. These include vertically dipping faults:

- to the south of the Ankom study area, along the E-W axis;
- between Viali and Doumé, running N-S;
- between Bika and Nlang, running NE-SW;
- and finally between Nlang and Mbangue, running NW-SE.

In addition to these vertically dipping faults, there are others that dip obliquely. These can be seen:

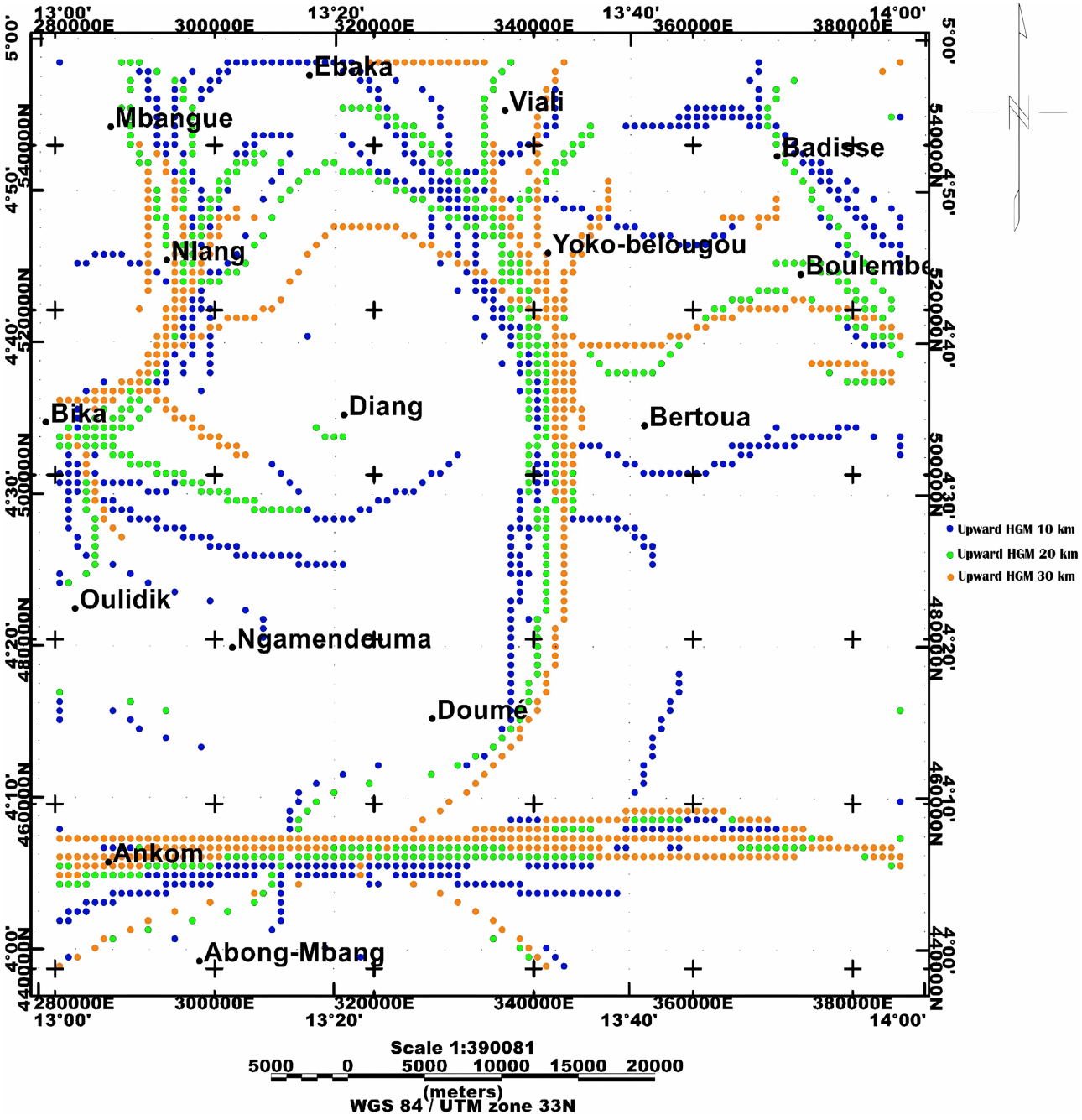

Figure 6. Superposition map of horizontal gradient maxima.

- to the south between Abong-Mbang and Ankom, trending ENE-WSW;
- Between Bika and Oudilik, there is an NW-SE accident;
- to the south of Boulembe, an ESE-WNW accident;
- and between Boulembe and Badissé, where there is an ESE-WNW accident;
- and from Yoko Betougou to Ebaka, with an ESE-WNW directional accident.

The lineament map (Figure 7(a)) is obtained by plotting the lineaments resulting from the superposition of the horizontal gradient maxima in Figure 6. These lineaments follow several structural directions, notably ESE-WNW, ENE-WSW,

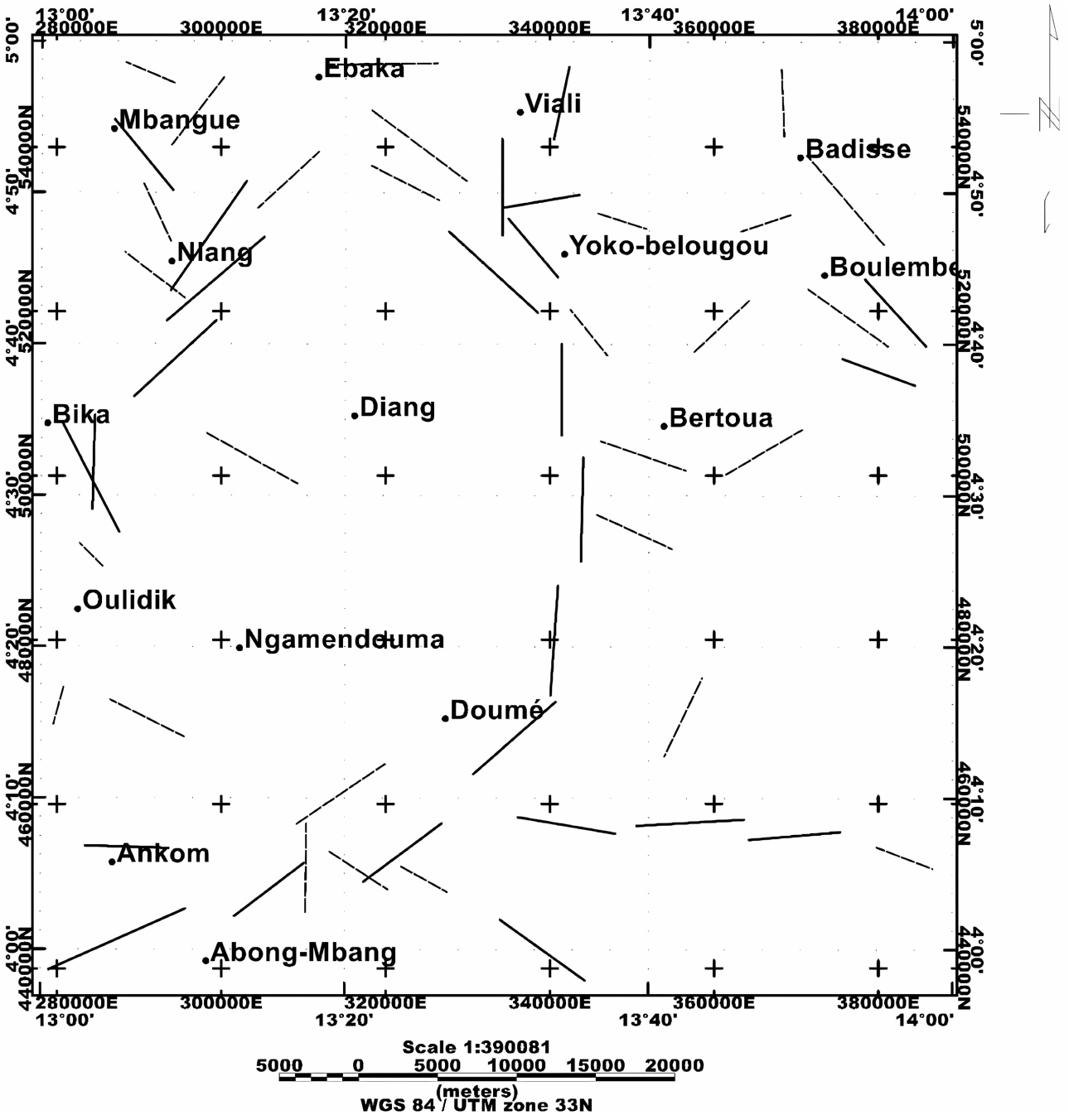

(a)

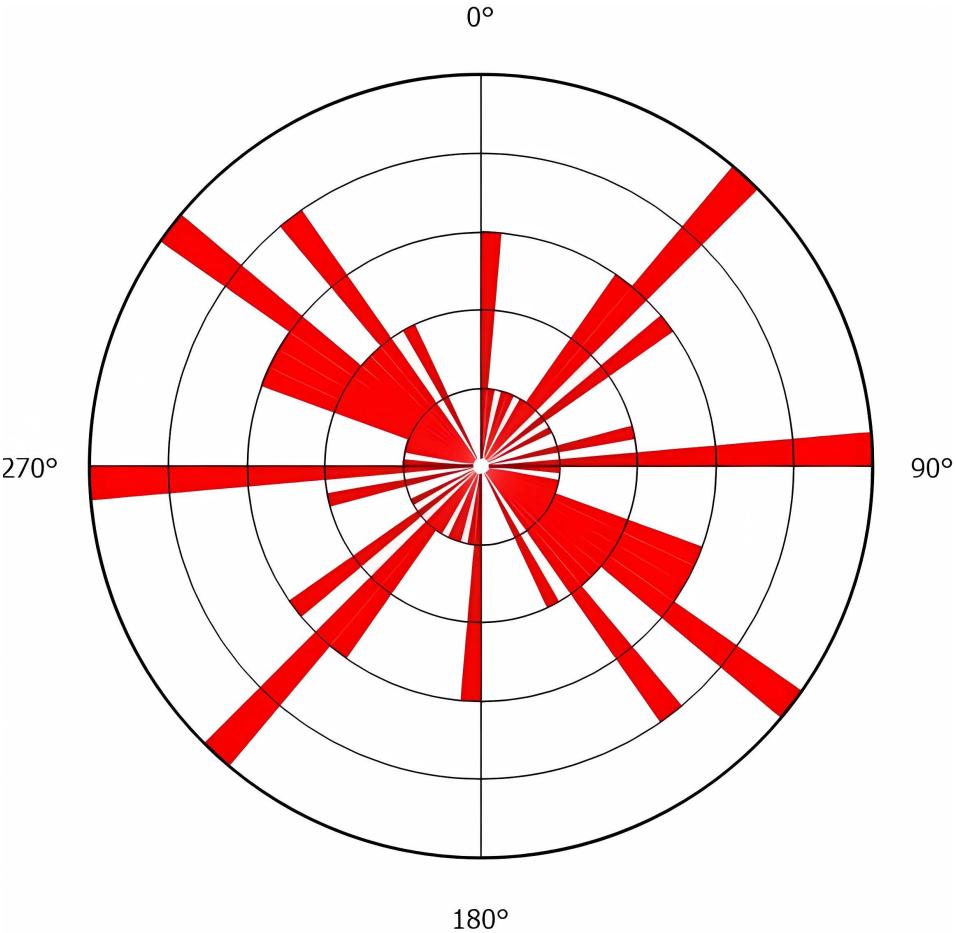

(b)

Figure 7. (a) Map of gravity lineaments. (b) Directional rosette of major and minor lineaments.

NW-SE, NE-SW, N-S and E-W. These directions are in good agreement, firstly with those observed in the analysis of the magnetic data, and secondly with the deformations observed on a regional scale, such as fractures, dykes and faults.

The map below (**Figure 7(b)**) shows the directional rosette of the various gravity lineaments. It shows that the lineaments preferentially follow NW-SE, ESE-WNW, NE-SW, ENE-WSW directions and, to a lesser extent E-W and N-S directions.

4.7. Quantitative Interpretation

This gives an idea of the depths of tectonic faults on the one hand, and on the other, an idea of the behaviour and lateral and vertical variations in the susceptibilities and densities of subsoil rocks.

4.7.1. Euler Deconvolution

Euler solutions were calculated using the following parameters: structural index 0, tolerance 10 and window size 15. The structural index 0 used here highlights the magnetic contacts observed in the study zone.

Analysis of the Euler solution map (**Figure 8**) highlights several tectonic faults.

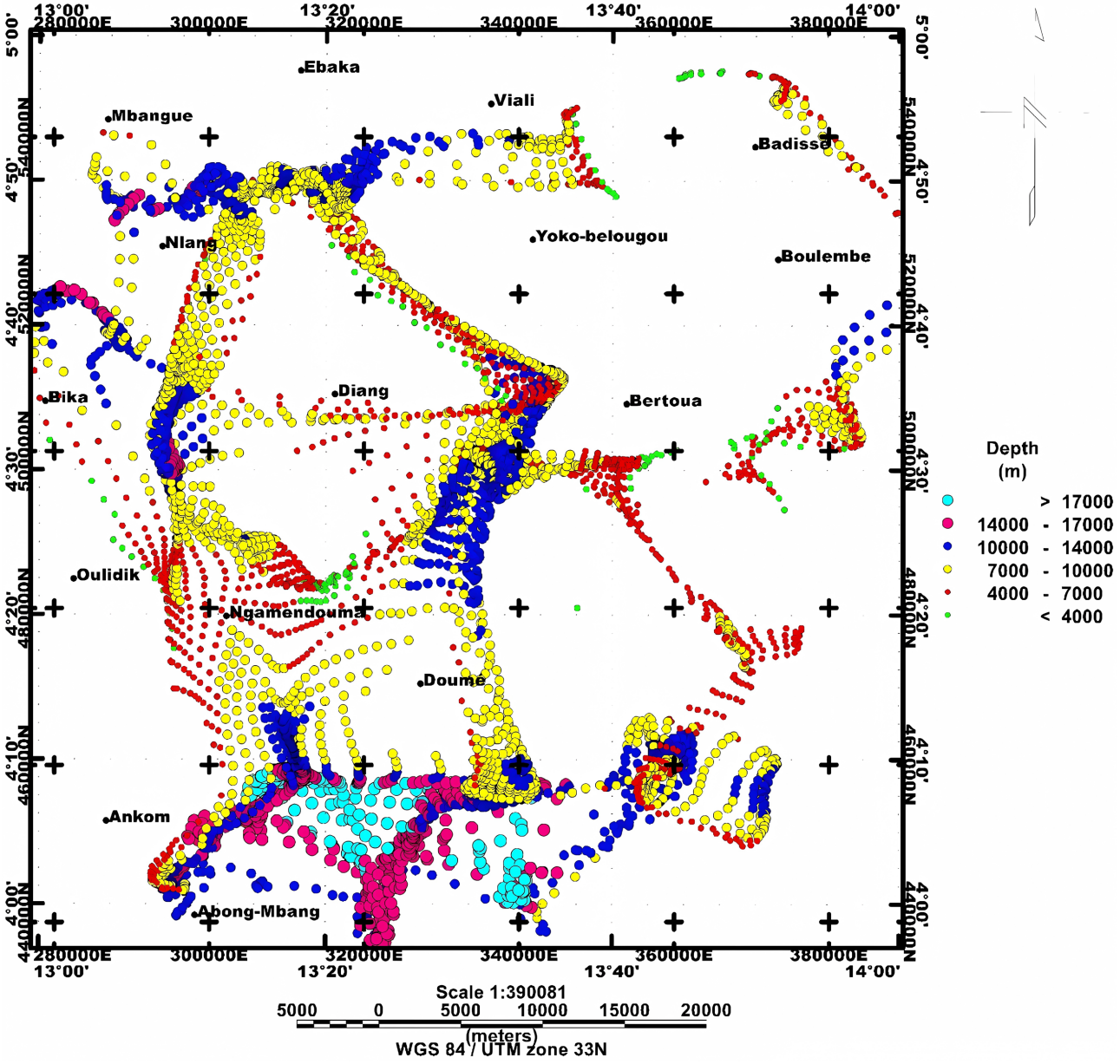

Figure 8. Map of Euler solutions.

It allows us to differentiate between intrusive bodies and deep faults. The shape of the groupings of Euler solutions confirms the tectonic faults mentioned in the previous maps on the one hand, and reveals new faults on the other.

To the south of the study area, particularly in the vicinity of Abong-Mbang, we note the presence of deep faults located at depths greater than 14 km and oriented ENE-WSW, ESE-WNW and NE-SW. The Oudilik-Ngamendouma zones are characterised by a swarm of shallow solutions that can be assimilated to intrusions.

The N-S-trending tectonic fault between Doumé and Diang mentioned in previous maps is still clearly defined here. It is thought to be located at depths greater than 7 km.

There is an NW-SE-oriented lineament between Bertoua and Mbangue, which

would indicate the presence of a 7 km deep fault, which extends to the south-east of the study area in the same direction. It appears to correlate well with the tectonic fault that divides the study area diagonally in the analysis of the previous magnetic data.

Between the villages of Nlang and Viali, there is an ENE-WSW fault 10 km deep. This fault was not mentioned in the aeromagnetic study. The Badissé area is crossed by an NW-SE tectonic fault that can be likened to a fracture.

4.7.2. Modelling $2^{3/4}$-D

Models can be used to observe lateral and vertical variations in rock density in the

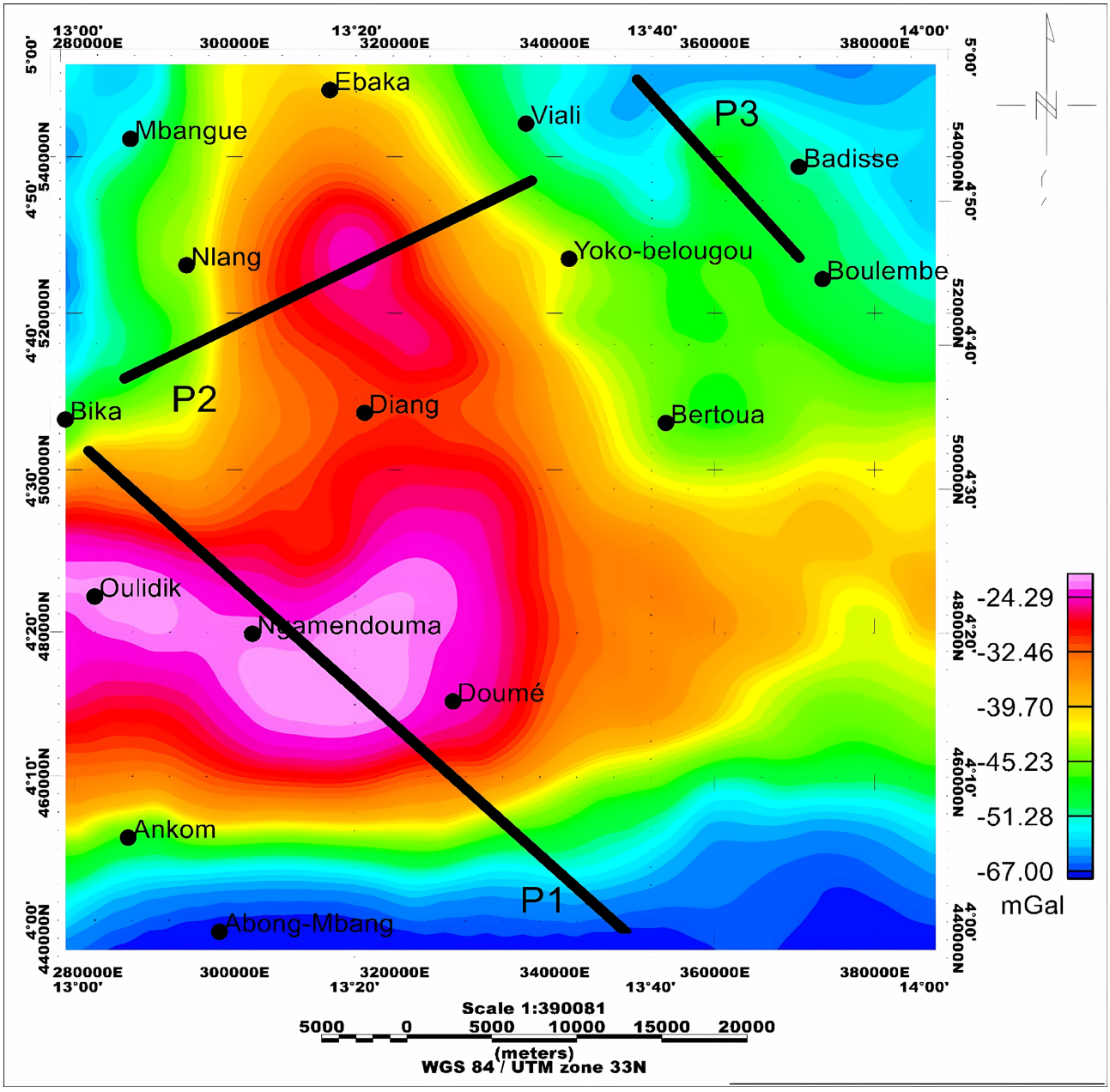

Figure 9. Bouguer anomaly map showing the profiles.

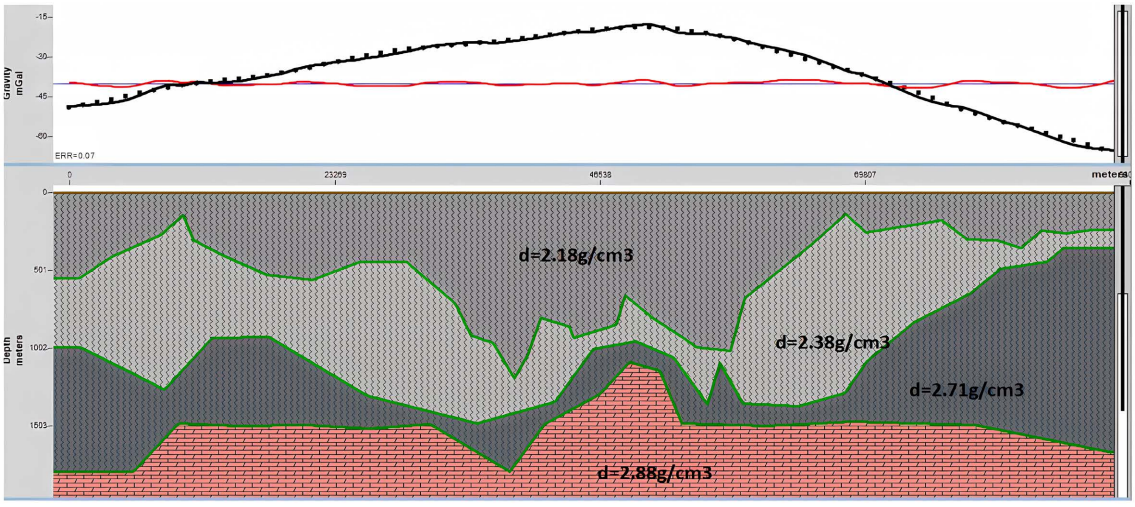

(a)

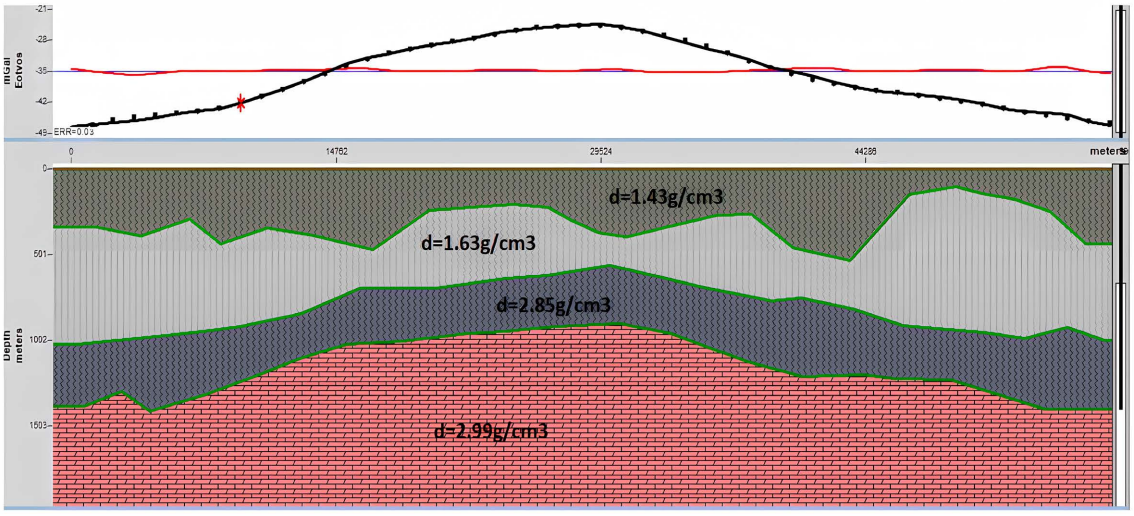

(b)

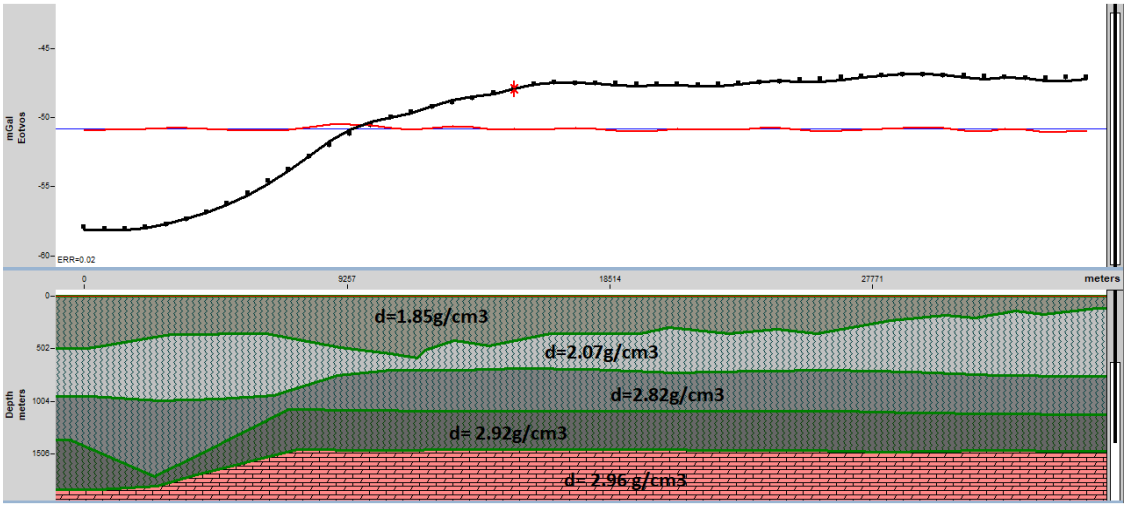

(c)

Figure 10. (a) Map of gravity profile 1. (b) Map of gravity profile 2. (c) Map of gravity profile 3.

subsurface. They can also be used to locate major discontinuities in the subsurface. The three gravity models plotted here each show highly deformed contours, bearing witness to intense folding, shearing and fracturing, proof that the area bears the imprint of the collision of two major geological units, namely the Pan-African formations and those of the Congo Craton. The figure opposite (**Figure 9**) is the Bouguer anomaly map showing the profiles.

Analysis of gravity profile P1

Gravity profile P1 (**Figure 10(a)**) runs NW-SE from the locality of Bika to the south of the study area, crossing the locality of Ngamendouma at the points (283316 m; 512299 m) and (341004 m; 440446 m). It is approximately 92 km long and centred on a zone of high anomalies. Gravimetric topography along this profile reveals four layers, including ancient and delayed tectonic granites, embrittled gneisses, two-mica gneisses and micaschists. The bedrock here is granitic. The $2^{3/4}$ D model of this gravity profile shows that it crosses a disturbed gravity relief with heavy to light gravity anomalies.

This profile has very irregular shapes which would correspond to intense folding or shearing with crushing of the structure's characteristic of a collision.

Analysis of gravity profile P2

Gravity profile P2 (**Figure 10(b)**) runs from Bika to Viali in an ENE-WSW direction, ending at coordinates (286651 m; 522869 m) and (344052 m; 532547 m). It is approximately 58 km long and centred on a zone of high anomalies. Gravimetric topography along this profile reveals four layers made up of syntectonic granites, biotite embrechites, two-mica gneisses and biotite gneisses. The bedrock here is granitic. The $2^{3/4}$-D model of this gravity profile shows that it crosses a disturbed gravity relief with heavy to light gravity anomalies.

This profile has very irregular shapes resembling deformed sinusoids, which would characterize the intensity of the folding that affected the study area.

Analysis of gravity profile P3

Gravity profile P3 (**Figure 10(c)**) runs from Boulembe to Viali in a NW-SE direction, ending at coordinates (369182 m; 520120 m) and (350770m; 550307m), is approximately 35 km long and is centred on a zone of high anomalies. Gravimetric topography along this profile reveals five layers, including ancient syntectonic granites, late syntectonic granites, late alkaline-tending granites, sericite-gneisses and embrechites. The bedrock here is granitic. The $2^{3/4}$ D model of this gravity profile shows that it crosses a disturbed gravity relief with moderate to slight gravity anomalies.

This profile shows a tabulation of the layers. The area near Viali is the one most affected by the tectonic movements that affected the basement, and is characterised by a contact between geological formations of different densities. It is thought to be the site of a major discontinuity assimilated to fracturing.

5. Discussion

The Bouguer anomaly map obtained here comes from EGM data (2008). It was

used to identify local and regional geological formations. It appears to correlate fairly well with the map obtained in the study by [50] and in the work of [1] [2]. This map highlighted several types of anomalies that led to the assumption of faults reflecting the subduction of the Pan-African Chain on the Congo Craton. This result correlates well with work carried out at both local and regional scales [45] [46] [48] [49].

The vertical gradient map highlights the discontinuities in the surface formations [23]. Several gradient zones can be seen, indicating the existence of a number of discontinuities linked either to the upwelling of heavy masses or to the passage of the Sanaga fault. The discontinuities observed in this map follow the directions recognised in the aeromagnetic work carried out by [45] [46] on a local scale and by several authors on a regional scale [23] [47]-[49].

Horizontal gradient maps can be used to identify contacts, faults, fractures and lithological boundaries [20]-[22]. They have highlighted several tectonic accidents, such as contacts/faults and material intrusions. These tectonic faults appear to be the result of the collision between the Congo Craton and the Pan-African Chain of Central Africa. These analyses can be correlated with several geophysical studies carried out both locally and regionally [16] [23] [45]-[48] [51].

The maps of the analytical signal and the tilt angle highlighted the major directions recognised both locally and regionally, and also revealed the presence of intrusive bodies with remarkable density contrasts, all of which correlate with the studies by [47] [52]. The geological faults observed here are probably associated with the subduction of the Pan-African into the Congolese Craton.

The Euler solution map was used to confirm the presence of fractures, faults, and intrusions in the subsurface, which are located at variable depths and are linked to shearing deformation and reflect the structural and tectonic aspects of the study area. The southern part of the study area stands out for the presence of faults over 17 km deep. These are located beneath the Craton at a contact between several geological formations. The various faults and fractures observed here seem to correlate well with the tectonic bundle constituting the dextral ductile to ductile-fragile detachment mentioned in the geological work of [4] [5] [53].

The $2^{3/4}$-D modelling of the gravity data made it possible to observe the behaviour of the geological structures at depth as observed in the gravity profiles plotted. The different profiles presented fairly disturbed gravity topographies that showed the different aspects of the anomalies. These profiles revealed intense folding and shearing in the subsurface, accompanied by the crushing of characteristic structures with the imprint of subduction of the Pan-African domain in the Congolese Craton. These analyses correlated well with those carried out both in geological work [6] [14] and in geophysical work carried out by [45] [46] [49] [52].

The filtering operations that led to the multi-scale analysis of the gravity data highlighted the major and minor geophysical lineaments. The results obtained in this work confirmed known deformations and highlighted new deformations. Indeed, the work of [54] interprets the geophysical lineaments as faults, fractures or

geological contacts. The various structural maps highlight several families of lineaments characterised by several structural directions, notably ESE-WNW, ENE-WSW, NW-SE, NE-SW, E-W, and N-S.

On a regional scale, the NW-SE lineaments seem to correlate with the crustal faulting that took place during the Pan-African orogeny and which corresponds to the boundary between the Pan-African chain of Central Africa and the Congo Craton, as observed in the work of [55]. The ENE-WSW anomalies seem to correlate with the directions of the Central Cameroon Shear as described in previous work by several authors such as [48], which also respect the direction of the gravity axis corresponding to the major fault of the Central Cameroon Shear. In general, the main directions observed in this study seem to correlate well with the NE-SW, NW-SE fault systems and the multiple deformations such as folds, fractures or faults proposed in the geophysical studies carried out by [51] [56]-[58] in the Akonolinga, Ayos and Abong-Mbang areas, [23] in the southern part of Cameroon on the one hand and in the geological studies carried out by [6] [53] in southern Cameroon, then [56] in the Awaé-Ayos area on the other.

The E-W anomalies are enhanced in the gravity study. The E-W faults are parallel to the orogenic belt squeezed between the Congo Craton and the Brazilian-Central African polycyclic complex [7] and to one of the phases of Pan-African deformation, in particular, the C3 dextral shear phase highlighted in the work of [6]

The N-S lineaments, which are also well enhanced in the gravimetric study, appear to be consistent with the tectonic lines highlighted in the work of [1] [2] and with the directions of the multiple foliations highlighted in the work of [14].

6. Conclusions

The structural map of the gravity lineaments was obtained using qualitative analysis. Contact zones, fractures, dykes and even faults were interpreted as zones. For its part, the quantitative study provided an opportunity to assess the depths at which the anomalies originated. The deepest anomalies are more than 17 km deep and lie to the south of the study area. Several regional anomalies were identified using Bouguer anomaly maps, which were closely linked to local and regional geological formations, as well as to several discontinuities.

The major results of this study have certainly contributed to improving geological and geophysical knowledge of the study area. The study area is thought to have been the site of intense tectonic movements, characterised by several linear structures with main directions ESE-WNW, ENE-WSW, NE-SW, NW-SE, and then secondary directions E-W and N-S. These linear structures are associated with faults, fractures, and various deformations, on the one hand, and circular anomalies, on the other, that are attributed to intrusions of strongly magnetic materials or granitic domes.

All these data highlighted in this study are in line with the geological and geophysical research carried out in the study area and on a regional scale. The study area, although theoretically located on the Pan-African chain, appears to have

traces of the Congolese Craton. The deep faults mapped in this work, therefore, seem to confirm the hypothesis of subduction of the Craton plate.

Acknowledgements

This work was carried out in the following institutions: the National Advanced School of Public Works of Yaoundé, Cameroon and the Advanced School of Mines Processing and Energy Resources of The University Bertoua, Cameroon. The authors would like to thank the editors and reviewers who undoubtedly helped to improve the quality of this work.

Data Availability

The corresponding author guarantees the availability of the data used to carry out this study.

Conflicts of Interest

The authors declare that there is no conflict of interest regarding the publication of this paper.

References

[1] Gazel, J. and Gérard, G. (1954) Notice explicative sur la feuille Batouri-Est. Direction des Mines, 43 p.

[2] Gazel, J. (1955) Notice explicative sur la feuille Batouri-Ouest. Direction des Mines, 44 p.

[3] Dumont, J.F. (1986) Identification par télédétection de l'accident de la Sanaga (Cameroun). Sa position dans les grands accidents d'Afrique Centrale et de la limite Nord du Craton du Congolais. *Géodynamique*, **1**, 13-19.

[4] Nzenti, J.P., Barbey, P., Macaudiere, J. and Soba, D. (1988) Origin and Evolution of the Late Precambrian High-Grade Yaounde Gneisses (Cameroon). *Precambrian Research*, **38**, 91-109. https://doi.org/10.1016/0301-9268(88)90086-1

[5] Ngako, V., Jegouzo, P. and Nzenti, J.P. (1991) Le cisaillement Centre Camerounais. Rôle structural et géodynamique dans l'orogénèse panafricaine. *Comptes Rendus de l'Académie des Sciences*, **313**, 457-463.

[6] Mvondo, H., Owona, S., Ondoa, J.M. and Essono, J. (2007) Tectonic Evolution of the Yaoundé Segment of the Neoproterozoic Central African Orogenic Belt in Southern Cameroon. *Canadian Journal of Earth Sciences*, **44**, 433-444. https://doi.org/10.1139/e06-107

[7] Eno Belinga, S.M. (1984) Géologie du Cameroun. Librairie Universitaire de Yaoundé, 307 p.

[8] Nzenti, J.P., *et al.* (1994) La Chaine Panafricaine au Cameroun: Cherchons suture et modèle. In: S.G.F., Ed., 15*è réunion des Sciences de la Terre*, Société Géologique de France, 99 p.

[9] Nzenti, J.P. (1998) Neoproterozoic Alkaline Meta-Igneous Rocks from the Pan-African North Equatorial Fold Bel (Yaounde, Cameroon): Biotitites and Magnetite Rich Pyroxenites. *Journal of African Earth Sciences*, **26**, 37-47. https://doi.org/10.1016/s0899-5362(97)00135-8

[10] Nzenti, J.P., Njiosseu, E.L.T. and Nzina, N.A. (2007) The Metamorphic Evolution of the Paleoproterozoic High Grade Banyo Gneisses (Adamawa, Cameroon, Central Africa). *Journal of African Earth Sciences*, **7**, 95-109.

[11] Tanko Njiosseu, E.L., Nzenti, J., Njanko, T., Kapajika, B. and Nédélec, A. (2005) New U-Pb Zircon Ages from Tonga (Cameroon): Coexisting Eburnean-Transamazonian (2.1 Ga) and Pan-African (0.6 Ga) Imprints. *Comptes Rendus. Géoscience*, **337**, 551-562. https://doi.org/10.1016/j.crte.2005.02.005

[12] Ganwa, A.A., Frisch, W., Siebel, W., Shang, C.K., Mvondo Ondoa, J., Satir, M., *et al.* (2008) Zircon $^{207}Pb/^{206}Pb$ Evaporation Ages of Pan-African Metasedimentary Rocks in the Kombé-II Area (Bafia Group, Cameroon): Constraints on Protolith Age and Provenance. *Journal of African Earth Sciences*, **51**, 77-88.

[13] Gazel, J., Houreq, C.Q.V. and Nickles, M. (1956) Notice explicative de la carte géologique au 1/1.000.000 du Cameroun. Bulletin Direction des Mines et de la Géologie Cameroun, No. 2, 62 p.

[14] Toteu, S.F., Penaye, J. and Djomani, Y.P. (2004) Geodynamic Evolution of the Pan-African Belt in Central Africa with Special Reference to Cameroon. *Canadian Journal of Earth Sciences*, **41**, 73-85. https://doi.org/10.1139/e03-079

[15] Nedelec, A., Macaudiere, J., Nzenti, J.P. and Barbey, P. (1986) Evolution structurale et métamorphisme des schistes de Mbalmayo (Cameroun). Information pour la structure de la zone mobile panafricaine d'Afrique Centrale au contact du Craton du Congo. *Compte Rendus Académie des Sciences*, *Paris*, **303**, 75-80.

[16] Manguelle-Dicoum, E., Bokosah, A.S. and Kwende-Mbanwi, T.E. (1992) Geophysical Evidence for a Major Precambrian Schist-Granite Boundary in Southern Cameroon. *Tectonophysics*, **205**, 437-446. https://doi.org/10.1016/0040-1951(92)90447-e

[17] Shandini, Y.N., Tadjou, J.M., Tabod, C.T. and Fairhead, J.D. (2010) Gravity Data Interpretation in the Northern Edge of the Congo Craton, South-Cameroon. *Anuário do Instituto de Geociências*, **33**, 73-82. https://doi.org/10.11137/2010_1_73-82

[18] Boukeke, D.B. (1994) Structures crustales d'Afrique Centrale déduites des anomalies magnétiques et gravimétriques: Le domaine Précambrien et du Sud-Cameroun. Thèse de Doctorat de Géophysique, Université Paris Sud, 263 p.

[19] Telford, W.M., Geldart, L.P., Sherriff, R.E. and Keys, D.A. (1990) Applied Geophysics. Cambridge Univ. Press, 860 p.

[20] Blakely, R.J. and Simpson, R.W. (1986) Approximating Edges of Source Bodies from Magnetic or Gravity Anomalies. *Geophysics*, **51**, 1494-1498. https://doi.org/10.1190/1.1442197

[21] Cordell, L. and Grauch, V.J.S. (1985) 16. Mapping Basement Magnetization Zones from Aeromagnetic Data in the San Juan Basin, New Mexico. In: Hinze, W.J., Ed., *The Utility of Regional Gravity and Magnetic Anomaly Maps*, Society of Exploration Geophysicists, 181-197. https://doi.org/10.1190/1.0931830346.ch16

[22] Phillips, J.D. (1998) Processing and Interpretation of Aeromagnetic Data for the Santa Cruz Basin-Patahonia Mountains Area, South-Central Arizona: U.S. Geological Survey Open-File Report 02-98.

[23] Feumoe, A.N.S., Ndougsa-Mbarga, T., Manguelle-Dicoum, E. and Derek-Fairhead, J. (2012) Delineation of Tectonic Lineaments Using Aeromagnetic Data for the Southeast Cameroon Area. *Geofizika*, **29**, 175-192.

[24] Gunn, P.J. (1975) Linear Transformations of Gravity and Magnetic Fields. *Geophysical Prospecting*, **23**, 300-312. https://doi.org/10.1111/j.1365-2478.1975.tb01530.x

[25] Nabighian, M.N. (1972) The Analytic Signal of Two-Dimensional Magnetic Bodies

with Polygonal Cross-Section: Its Properties and Use for Automated Anomaly Interpretation. *Geophysics*, **37**, 507-517. https://doi.org/10.1190/1.1440276

[26] Nabighian, M.N. (1974) Additional Comments on the Analytic Signal of Two-Dimensional Magnetic Bodies with Polygonal Cross-Section. *Geophysics*, **39**, 85-92. https://doi.org/10.1190/1.1440416

[27] Nabighian, M.N. (1984) Toward a Three-Dimensional Automatic Interpretation of Potential Field Data via Generalized Hilbert Transforms: Fundamental Relations. *Geophysics*, **49**, 780-786. https://doi.org/10.1190/1.1441706

[28] Rasolomanana, E., Andriamirado, L.C., Randrianja, R. and Ratefiarimino, A. (2010) Analyse et interprétation des données aéromagnétiques et spectrométriques de la région d'Andriamena. *Madamines*, **1**, 1-14.

[29] Roest, W.R., Verhoef, J. and Pilkington, M. (1992) Magnetic Interpretation Using the 3-D Analytic Signal. *Geophysics*, **57**, 116-125. https://doi.org/10.1190/1.1443174

[30] Miller, H.G. and Singh, V. (1994) Potential Field Tilt—A New Concept for Location of Potential Field Sources. *Journal of Applied Geophysics*, **32**, 213-217. https://doi.org/10.1016/0926-9851(94)90022-1

[31] Verduzco, B., Fairhead, J.D., Green, C.M. and MacKenzie, C. (2004) New Insights into Magnetic Derivatives for Structural Mapping. *The Leading Edge*, **23**, 116-119. https://doi.org/10.1190/1.1651454

[32] Salem, A., Williams, S., Fairhead, D., Smith, R. and Ravat, D. (2008) Interpretation of Magnetic Data Using Tilt-Angle Derivatives. *Geophysics*, **73**, L1-L10. https://doi.org/10.1190/1.2799992

[33] Bouiflane, M. (2008) Cartographie aéromagnétique et magnétique multi-échelles: Etude structurale d'une région du Fossé Rhénan. Thèse de Doctorat de Géophysique, Université Louis Pasteur-Strasbourg I, 206 p.

[34] Muzaffer, Ö. and Ünal, D. (2013) Edge Detection of Magnetic Sources Using Enhanced Total Horizontal Derivative of the Tilt Angle. *Bulletin of the Earth Sciences Application and Research Centre of Hacettepe University*, *Yerbilimleri*, **34**, 73-82.

[35] Vanié, L.T.A., Khattach, D. and Houari, M.R. (2005) Apport des filtrages des anomalies gravimétriques à l'étude des structures profondes du Maroc oriental. *Bulletin Institut des Sciences de Rabat*, *Section Sciences de la Terre*, **27**, 29-40.

[36] Khattach, D., Keating, P., Mili, E.M., Chennouf, T., Andrieux, P. and Milhi, A. (2004) Apport de la gravimétrie à l'étude de la structure du bassin des Triffa (Maroc nord-oriental): Implications hydrogéologiques. *Comptes Rendus. Géoscience*, **336**, 1427-1432. https://doi.org/10.1016/j.crte.2004.09.012

[37] Khattach, D., Mraoui, H., Sbibih, D. and Chennouf, T. (2006) Analyse multi-échelle par ondelettes des contacts géologiques: Application à la carte gravimétrique du Maroc nord-oriental. *Comptes Rendus. Géoscience*, **338**, 521-526. https://doi.org/10.1016/j.crte.2006.03.002

[38] Reid, A.B., Allsop, J.M., Granser, H., Millett, A.J. and Somerton, I.W. (1990) Magnetic Interpretation in Three Dimensions Using Euler Deconvolution. *Geophysics*, **55**, 80-91. https://doi.org/10.1190/1.1442774

[39] Thompson, D.T. (1982) EULDPH: A New Technique for Making Computer-Assisted Depth Estimates from Magnetic Data. *Geophysics*, **47**, 31-37. https://doi.org/10.1190/1.1441278

[40] El Goumi, N., Jaffal, M., Kchikach, A. and Manar, A. (2010) Contribution of the Gravimetry to the Structural Study of the Haouz (Morocco). *Estudios Geológicos*, **66**, 181-191. https://doi.org/10.3989/egeol.40051.082

[41] Talwani, M. and Heirzler, J.R. (1964) Computation of Magnetic Anomalies Caused by Two-Dimensional Bodies or Arbitrary Shape. Computers in the Mineral Industry, School of Earth Sciences, Standford University, 210 p.

[42] Visweswara Rao, C., Raju, M.L. and Chakravarthi, V. (1995) Gravity Modelling of an Interface above Which the Density Contrast Decreases Hyperbolically with Depth. *Journal of Applied Geophysics*, **34**, 63-67. https://doi.org/10.1016/0926-9851(94)00057-u

[43] Cooper, G.R.J. (2003) Grav2dc. 2.10. An Interactive Gravity Modeling Program for Microsoft Windows. University of the Witwatersrand.

[44] Pavlis, N.K., Holmes, S.A., Kenyon, S.C. and Factor, J.K. (2008) An Earth Gravitational Model to Degree 2160: EGM2008. *The EGU General Assembly*, Vienna, 13-18 April 2008.

[45] Owono Amougou, O.U.I., Ndougsa-Mbarga, T., Meying, A., Assembe, S.P., Ngoh, J.D., Ngoumou, P.C. and Yandjimain, J. (2019) Evidence of Major Structural Features over the Pan-African Domain in the Bertoua-Mbangue Area (East Cameroon) from a Multiscale Approach of Modeling and Interpretation of Aeromagnetic Data. *International Journal of Geophysics*, **2019**, Article ID: 9148678.

[46] Owono Amougou, O.U.I., Ndougsa Mbarga, T., Meying, A., Abate Essi, J.M., Mono, J.A., Manvele, D.P., *et al.* (2020) Interpretation of Aeromagnetic Data to Investigate Crustal Structures of the Contact Congo Craton—Pan-African Belt at the Eastern Cameroon. *Earth Science Research*, **9**, 48. https://doi.org/10.5539/esr.v9n2p48

[47] Ndougsa Mbarga, T., Feumoe, A.N., Manguelle-Dicoum, E. and Derek Fairhead, J. (2012) Aeromagnetic Data Interpretation to Locate Buried Faults in South-East Cameroon. *Geophysica*, **48**, 49-63.

[48] Tatchum, C.N., Tabod, C.T. and Manguelle-Dicoum, E. (2006) A Gravity Study of the Crust beneath the Adamawa Fault Zone, West Central Africa. *Journal of Geophysics and Engineering*, **3**, 82-89. https://doi.org/10.1088/1742-2132/3/1/009

[49] Zanga Amougou, A., Ndougsa Mbarga, T., Meying, A., Layu Yufenyu, D., Bikoro Bi Alou, M. and Manguelle Dicoum, E. (2013) 2.5 D Modeling of Crustal Structures along the Eastern Cameroon and Western Central African Republic Derived from Finite Element and Spectral Analysis Methods. *Geophysica*, **49**, 75-97.

[50] Poudjom Djomani, Y.H. (1993) Apport de la gravimétrie à l'étude de la lithosphère continentale et implications géodynamiques. Etude d'un bombement intraplaque: Le massif de l'Adamaoua (Cameroun). Thèse de Doctorat, Université de Paris XI Orsay, 229 p.

[51] Meying, A., Mbarga, T.N., Gouet, D. and Stéphane, P.A. (2013) Near Surface Fractures Evidence from Audio-Magnetotelluric (AMT) Investigation in Ayos-Nguelemendouka Area (Eastern Cameroon). *International Journal of Geosciences*, **4**, 480-493. https://doi.org/10.4236/ijg.2013.42045

[52] Mono, J.A., Bouba, A., Amougou, O.U.I.O., Ngoh, J.D., Nyam, F.M.E.A. and Mbarga, T.N. (2024) Analysis of Aeromagnetic Data for Enhancing Geologic Features Using Filtering Techniques over the Congo Craton-Pan-African Belt Contact, Centre-East Cameroon. *International Journal of Geophysics*, **2024**, Article ID: 4767612. https://doi.org/10.1155/2024/4767612

[53] Mvondo, H., Essono, J., Mvondo Ondoa, J. and Yene Atangana, J.Q. (2007) Comment on U-Pb Dating of Plutonic Rocks Involved in the Nappe Tectonic in Southern Cameroon: Consequence for the Pan-African Orogenic Evolution of the Central African Fold Belt. *Journal of African Earth Sciences*, **44**, 479-493.

[54] Koumetio, F., Njomo, D., Tabod, C.T., Noutchogwe, T.C. and Manguelle-Dicoum, E.

(2012) Structural Interpretation of Gravity Anomalies from the Kribi-Edea Zone, South Cameroon: A Case Study. *Journal of Geophysics and Engineering*, **9**, 664-673. https://doi.org/10.1088/1742-2132/9/6/664

[55] Basseka, C.A., Shandini, Y. and Tadjou, J.M. (2011) Subsurface Structural Mapping Using Gravity Data of the Northern Edge of the Congo Craton, South Cameroun. *Geofizika*, **28**, 229-245.

[56] Ndougsa-Mbarga, T., Manguelle-Dicoum, E., Tabod, C.T. and Mbom-Abane, S. (2003) Modelisation d'anomalies gravimétriques dans la région de Mengueme-Akonolinga (Cameroun). *Science, Technologie et Développement*, **10**, 67-74.

[57] Ndougsa Mbarga, T., Meying, A., Bisso, D., Layu, D.Y., Sharma, K.K. and Manguelle-Dicoum, E. (2011) Audiomagnetotellurics (AMT) Soundings Based on the Bostick Approach and Evidence of Tectonic Features along the Northern Edge of the Congo Craton, in the Messamena/Abong-Mbang Area (Cameroon). *The Journal of Indian Geophysical Union*, **15**, 145-159.

[58] Meying, A., Ndougsa-Mbarga, T. and Manguelle-Dicoum, E. (2009) Evidence of Fractures from the Image of the Subsurface in the Akonolinga-Ayos Area (Cameroon) by Combining the Classical and the Bostick Approaches in the Interpretation of Audio-Magnetotelluric Data. *Journal of Geology and Mining Research*, **1**, 159-171.